A Dynamic Structure for the Acyl−Enzyme Species of the Antibiotic Aztreonam with the *Citrobacter freundii* β-Lactamase Revealed by Infrared Spectroscopy and Molecular Dynamics Simulations†

Alan-Shaun Wilkinson,‡ Patrick K. Bryant,‡ Samy O. Meroueh,§ Malcolm G. P. Page,|| Shahriar Mobashery,*,§ and Christopher W. Wharton*,‡

School of Biosciences, University of Birmingham, Birmingham B15 2TT, United Kingdom, Department of Chemistry and Institute for Drug Design, Wayne State University, Detroit, Michigan 48202-3489, and Basilea Pharmaceutica, CH-4070 Basel, Switzerland

Received August 21, 2002; Revised Manuscript Received December 19, 2002

ABSTRACT: Infrared difference spectra show that at least 4 conformations coexist for the ester carbonyl group of the stable acyl−enzyme species formed between the antibiotic aztreonam and the class C β-lactamase from *Citrobacter freundii*. A novel method for the assignment of the bands that arise from the ester carbonyl group has been employed. This has made use of the finding that the infrared absorption intensity of aliphatic esters is surprisingly constant, so a direct comparison with simple model esters has been possible. This has allowed a clear distinction to be made between ester and amide (protein) absorptions. The polarity of the conformer environment varies from hexane-like to strongly hydrogen-bonded. We assume that the conformer with the lowest frequency (1690 cm^{-1}) and hence the strongest hydrogen-bonding is the singular conformer observed in the X-ray crystallographic structure, since a good interaction via two hydrogen bonds with the oxyanion hole is seen. Molecular dynamics simulation by the method of locally enhanced sampling revealed that the motion of the ester carbonyl of the acyl−enzyme species in and out of the oxyanion hole is facile. The simulation revealed two pathways for this motion that would go through intermediates that first break one or the other of the two hydrogen bonds to the oxyanion hole, prior to departure of the carbonyl moiety out of the active site. It is likely that such motion for the acyl−enzyme species might also occur with more typical β-lactam substrates for β-lactamases, but their detection in the more rapid time scale may prove a challenge.

The question as to how well X-ray crystallographic structures represent the dynamic state of protein−ligand complexes in solution has been much debated. The question has been partly answered by comparison of crystallographic and NMR structures of stable complexes, such as trypsin-inhibitor complexes (*1*). Studies such as these have shown a general agreement between the techniques, although structures deduced from NMR data perhaps show mobility/dispersion more graphically. Loop motion is often dramatically portrayed. While there are now many reports in the literature concerning multiple conformations of amino acid side chains and larger scale conformational changes in proteins, there is very little in the literature concerning ligand conformational multiplicity (*2*−*6*). One well-studied case is that of dihydrofolate reductase with methotrexate bound (*7*, *8*). The ligand clearly resides in two conformations. It is not clear what, if any, mechanistic significance this carries, since it is a synthetic inhibitor and not a substrate.

Conformational flexibility in the course of catalysis (*9*−*17*) and inhibition (*18*, *19*) has been documented for β-lactamases as well. It is critical that structural information be put in the context of the documented conformational changes to arrive at the details of the catalytic processes by these enzymes.

Catalysis by serine-dependent β-lactamases proceeds via a two-step mechanism that involves acylation of the active site serine and the deacylation of the acyl−enzyme species (*20*). Binding of the substrate at the Michaelis complex stage involves sequestration of the β-lactam carbonyl in what is referred to as the oxyanion hole. The oxyanion hole donates two hydrogen bonds to the β-lactam carbonyl, inducing polarization, to facilitate acylation of the active site serine. The hydrolytic processing of the ester moiety in the second step of catalysis also benefits from the polarization induced by the two hydrogen bonds within the oxyanion hole (see Figure 1). Hence, the mechanistic contribution of the oxyanion hole is potentially substantial.

Infrared spectroscopy was recently used to measure the carbonyl stretch frequencies of the acyl−enzyme species that form in hydrolysis of methicillin by the class C β-lactamase from *Citrobacter freundii*, a potent urinary tract pathogen in hospitals (*6*). The spectra were interpreted to show that there are at least 4 acyl−enzyme conformations and that the

† This work was supported by the BBSRC, U.K., Basilea Pharmaceutica, and F. Hoffmann-La Roche Ltd. (to C.W.W.) and by the National Institutes of Health (to S..M.).

* To whom correspondence should be addressed. E-mail: c.w.wharton@bham.ac.uk (C.W.W.); som@chem.wayne.edu (S.M).

‡ University of Birmingham.

§ Wayne State University.

|| Basilea Pharmaceutica.

10.1021/bi0266941 CCC: $25.00
Published on Web 01/28/2003

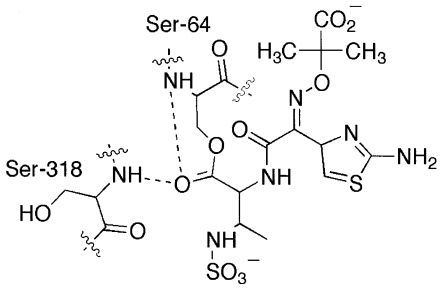

FIGURE 1: Schematic rendering of the acyl−enzyme species, as seen in the X-ray structure (*21*).

ester carbonyl groups in these species experienced a wide range of intra-active site environments, from hydrophobic to very polar. There is no crystallographic structure of the methicillin−*C. freundii* β-lactamase acyl−enzyme, so it was not possible to make a comparison between crystal and solution structures with the same ligand.

Aztreonam was the first fully synthetic monocyclic β-lactam antibiotic and is highly resistant to hydrolytic turnover by most β-lactamases because its deacylation is slow (*21*). The X-ray crystallographic structure of the complex of aztreonam with the *C. freundii* β-lactamase has been determined, since the acyl−enzyme intermediate is sufficiently stable (*21*). A single conformer of the acyl group has been modeled to fit the electron density. This conformer shows a well-formed bifurcated hydrogen-bonding interaction with the oxyanion hole; see Figure 1.

We report herein on the conformational flexibility of the ester carbonyl of the acyl−enzyme species formed between the clinically used aztreonam and the class C β-lactamase from *C. freundii*. The dynamic nature of these events is documented by molecular dynamics simulations of the acyl−enzyme species, which provide for the first time a structural basis for our experimental observations by infrared spectroscopy.

MATERIALS AND METHODS

Aztreonam was supplied by ICN Pharmaceuticals, Thame, Oxfordshire, U.K. Deuterium oxide (99%) was supplied by Aldrich, Gillingham, Dorset, U.K. All other chemicals were supplied by either Aldrich or Sigma, U.K.

The *C. freundii* (*Escherichia coli* Amp C type) was prepared as previously described (*21*). For IR experiments the enzyme (5 mL, in 50% glycerol) was concentrated using an Amicon pressure dialyzer to 0.5 mL. The solution was diluted to 5 mL with 0.1 M phosphate buffer pM[1] 7.0, made up in deuterium oxide, and reconcentrated to 0.5 mL. This procedure was repeated twice more before the enzyme was freeze-dried. Prior to IR experiments the enzyme was made up to 0.5 mL with 0.1 M sodium phosphate buffer as above and incubated for 72 h at 4° to allow extensive hydrogen−deuterium exchange.

Infrared Spectroscopy of Model Compounds. The spectra of model esters were measured as 1 or 2% solutions in hexane, in acetonitrile, and where possible in deuterium oxide. The solvent was used as the reference against which the sample spectra were ratioed. The spectra of a wide range of aliphatic ethyl and methyl esters were measured including α,β-unsaturated esters. Model esters used were the following: methyl acetate; ethyl acetate; ethyl cinnamate; methyl β-phenylpropionate; ethyl β-phenylpropionate; phenylalanine ethyl ester (not measured in hexane). The spectra of a few aromatic esters were also measured, and it was apparent that aromatic ester carbonyl groups show both molar absorbances and absorption frequencies that are distinct from those of the aliphatic ester family; these were thus excluded from further consideration.

Infrared Spectroscopy Experiments: Enzyme Measurements. To measure the acyl−enzyme single beam spectrum, 10 μL of 5 mM aztreonam solution made up in deuterated phosphate buffer, as above, was added to 90 μL of 0.43 mM enzyme solution in deuterated phosphate buffer. This solution was then injected into the "in situ" cuvette, which has a path length of 100 μm enclosed by CaF_2 windows and separated by a Teflon spacer. Use of an in situ cuvette obviates the need to open the spectrometer and greatly reduces the problem of water vapor bands being present in sensitive difference spectra. The reference (enzyme) single beam spectrum was measured as above by replacing the aztreonam solution with phosphate buffer in deuterium oxide. For both the acyl−enzyme and reference enzyme single-beam spectra, a set of 33 × 256 scans were collected, centered upon 1 min intervals, using a Bruker IFS 66 spectrometer with a scan rate of 17 s^{-1} (180 kHz) and a resolution of 2 cm^{-1}. Multiple data sets were accumulated as described above over a period of time, so that they could be examined for kinetic changes, e.g. slow conformational changes, during the course of the experiment. As described below, there were none discernible. Collection of the enzyme reference spectrum in this way allows for partial compensation of residual hydrogen−deuterium exchange that usually occurs during the course of an experiment. To construct the difference spectrum, the acyl−enzyme single beam spectrum was divided by the reference single beam spectrum before conversion to absorbance. To check that water vapor bands did not interfere with the difference spectra, a water vapor spectrum was superimposed on the difference spectrum of Figure 2 to ensure that there was no coincidence of bands. Minor baseline corrections were made to compensate for instrument baseline drift during the course of an experiment, but no other mathematical manipulations were performed upon the data other than coaddition and averaging of the data sets.

An alternative analysis involved subtracting the last difference spectrum (33 min) from all others. This showed that no kinetic trends occurred in the intensities of the several bands in the spectra from the time of the first spectrum 40 s after mixing to the end of the experiment at 33 min. There were small variations in the apparent band structure, i.e., in the apparent number of subcomponents of overlapping bands, in individual sets of 256 scans. When the results of four complete experiments (i.e. 132 × 256 scans) were averaged, these uncertainties were clearly resolved to show that each component of the difference spectrum was well fitted by a single Gaussian with little or no Lorentzian character. Thus acylation of the enzyme was complete and essentially quantitative (see below) after 40 s. Band-fitting was achieved by using the Bruker Opus software as was band integration. It is apparent (Figure 2) that the fit is very good owing to good band separation and low noise. The low noise apparent in Figure 2 is the result of the combination of four separate complete experiments to give a total of 33 792 scans in both the sample and reference spectra. There are no bands in the

IR spectrum of aztreonam in deuterated phosphate buffer between that at 1762 cm^{-1} (β-lactam carbonyl) and 1650 cm^{-1} (amide).

Computational Procedures and Molecular Dynamics Simulations. The X-ray structure of the acyl−enzyme species aztreonam−*C. freundii* β-lactamase (accession number 1FR6) was obtained from the Research Collaboratory for Structure Bioinformatics database (http://www.rcsb.org/pdb/ index.html). The enzyme was protonated using the program Protonate of the AMBER 7 suite of programs (*22*). Atomic charges for aztreonam were computed using the RESP fitting procedure (*23*). A HF/6-31G* single-point energy calculation was used to determine the electrostatic potential around the molecule, which was subsequently used in the two-stage RESP fitting procedure. All ab initio calculations were carried out using the Gaussian 98 suite of programs (*24*). The acyl−enzyme complex was then immersed in a box of TIP3P water with at least 10 Å between any face of the box and the enzyme. The solvated acyl−enzyme species consisted of approximately 60 000 atoms. Preparation of the complexes for molecular dynamics simulations was based on a protocol described previously (*25*), except that in this study equilibration at 300 K was carried out for 270 ps. The particle mesh Ewald (PME) method was used to treat long-range electrostatics (*26*). Bonds that involved hydrogen atoms were constrained with the SHAKE algorithm and a time step of 2 fs was used to carry out molecular dynamics simulations (*27*). All non-locally enhanced sampling (LES) energy minimizations and molecular dynamics simulations of the solvated acyl−enzyme intermediate were carried out using the Sander module within the AMBER 7 suite of programs (*22*). Forcefield parameters and atomic charges for standard protein residues were obtained from the "parm99" set of parameters.

The program Sander.LES, which is part of the AMBER 7 package, was used to carry out all locally enhanced sampling (LES) simulations. Setup of the LES simulations closely followed previously described simulations (*28*). After equilibration, the resulting topology and coordinate files were converted to LES-ready files using the Addles program. The LES system consisted of the solvated acyl−enzyme intermediate from above, except that five copies of the Ser-64 bound to aztreonam were made. A total of 1.8 ns of LES simulations was carried out.

RESULTS AND DISCUSSION

Aztreonam is a clinically used β-lactam antibiotic of a unique structure. Its structure contains a single β-lactam ring (a monobactam), as opposed to fused rings for penicillins, cephalosporins, and carbapenems (Scheme 1). Acylation of the *C. freundii* β-lactamase by aztreonam is rapid (*29*). An additional feature of structural difference is the presence of the sulfonyl group on the ring of aztreonam; the negative charge is proposed to interact with Lys-315 in the Michaelis complex but not in the acyl−enzyme species. Additionally, the presence of the C-4 methyl group hinders rotation in the ring-opened form (*30*). Figure 2 shows the difference spectrum of the aztreonam acyl−enzyme species formed with the *C. freundii* β-lactamase. Table 1 presents the frequency maxima, bandwidths, integrated intensities, and assignments of the various bands shown in Figure 2. Perusal of Figure 2 and Table 1 reveal that both the aztreonam and methicillin

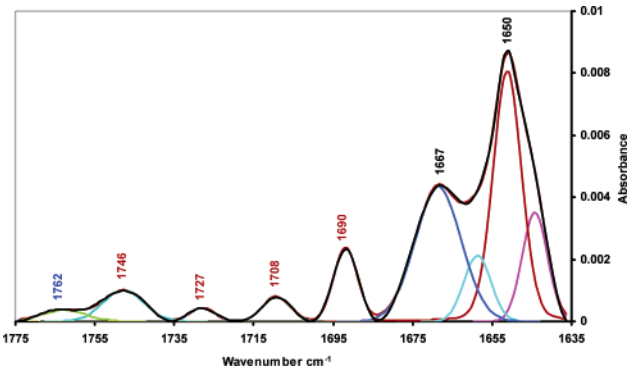

FIGURE 2: IR difference spectrum of the acyl−enzyme formed by acylation of *C. freundii* β-lactamase with aztreonam. The spectral data were gathered at 22° in 0.1 M phosphate buffer made up in deuterium oxide and adjusted to an apparent pH (pM) of 7.0. The final spectrum represents the combination, by coaddition, of four complete experiments as described in Materials and Methods. Band-fitting was achieved by using the Bruker Opus software. The experimental spectrum is shown in black, while the (largely superimposed) band-fitted line is shown in red. Spectral parameters and assignments are collected in Table 1.

Scheme 1: Structures of Aztreonam (Left) and Methicillin (Right)

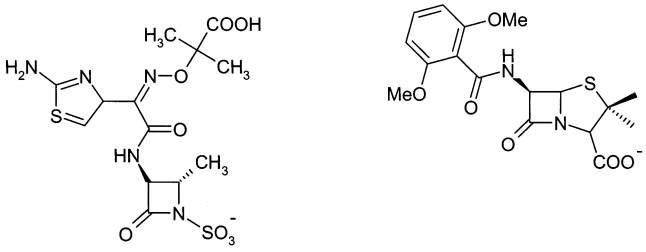

acyl−enzymes species display multiple features in the ester carbonyl stretch region, including some bands that extend into the region (1700−1600 cm^{-1}) in which amide carbonyl stretch vibrations of the various protein secondary structures occur.

Use of Model Esters in the Assignment of the Acyl−Enzyme Carbonyl Bands. When multiple bands are observed and isotope editing is not used to provide definitive assignments of band origins, it is uncertain how many of these bands may be assigned with confidence to acyl−enzyme ester carbonyl stretch vibrations rather than to perturbed carboxyl groups or perturbations in protein structure. One approach to assignment is to consider only the frequencies of the bands, but this is not robust since the absorption bands can overlap. Bands that arise from protein perturbations can overlap with strongly hydrogen-bonded ester carbonyl vibrations in the high-frequency region of protein perturbations (1670−1700 cm^{-1}). The absorption of the protonated form of carboxyl groups with pK_a values that are perturbed on ligand interaction can overlap with the normal frequency range for ester vibrations (1700−1750 cm^{-1}); see below. A novel approach to assignment uses the band intensities of model spectra, determined in pure solvents. This approach, adopted here, proves to be quite robust since the integrated absorption intensities of (most) ester carbonyl groups are surprisingly invariant with structure. They do however vary somewhat with solvent dielectric and more strongly when hydrogen bonding to the carbonyl group can occur. This

Table 1: Analysis of the Ester Carbonyl Absorption Bands of the *C. freundii* β-Lactamase Acyl−Enzyme Complex

wavenumber, cm^{-1}	bandwidth,[b] cm^{-1}	$10^3 \times$ integrated intensity[b]	cumulative intensity	assgnt
1762	13[c]	0.6	0.6[d]	excess aztreonam
1746 (1737)[a]	12	5.7	5.7	acyl−enzyme >C═O 1
1727 (1727)[a]	7	1.5	7.2	acyl−enzyme >C═O 2
1708 (1707)[a]	8	2.6	9.8	acyl−enzyme >C═O 3
1690 (1683)[a]	7	7.9	17.7, 21,[e] 14.8[f]	acyl−enzyme >C═O 4
1667	14	21.0	39.3	change in turns (loops)[g]
1657	8	4.1	43.4	α-helix perturbation[g]
1650	7	29.0	72.4	random coil (loop) perturbation[g]
1642	8	6.6	79	β-sheet perturbation[g]

[a] Frequencies of the methicillin−*C. freundii* acyl−enzyme complex. [b] The bandwidths and integrated intensities were measured by band-fitting. [c] The bandwidth of aztreonam seen in Figure 2 is abnormally narrow (normally 35 cm^{-1} in free solution) and may be the result of interaction with the protein or an artifact owing to the small size of the band. [d] The aztreonam contribution is not included in the cumulative sum shown below. [e] The mean intensity of model esters (see Table 2) in hexane. [f] The mean intensity of model esters in deuterium oxide. [g] See ref 36.

Table 2: Effect of Solvent Dielectric Constant upon the Absorption Band Properties of Model Esters

solvent	integrated abs of ester carbonyl band (±SD)	bandwidth at half-height, cm^{-1} (±SD)
hexane[a]	49 ± 4	9 ± 1.6
acetonitrile[b]	46 ± 1	14.4 ± 1.4
deuterium oxide[c]	34 ± 0.5	25 ± 2.2

[a] Model esters used: ethyl acetate; ethyl cinnamate; ethyl hydrocinnamate; ethyl propionate. [b] Model esters used: ethyl acetate; ethyl cinnamate; ethyl hydrocinnamate; L-phenylalanine ethyl ester. [c] Model esters used: aztreonam ethyl ester; L-phenylalanine ethyl ester; monoethyl succinate. Spectra were measured on 2% solutions in hexane and acetonitrile and 40 mM solutions in unbuffered deuterium oxide. Band parameters were determined as described for Figure 2.

approach allows us to estimate how many of the bands seen in Figure 2 can be accounted for by the predicted total intensity, calculated from the concentration of the acyl−enzyme, by using Beer's law.

This approach does not eliminate the possibility that one or more bands may arise from carboxyl group perturbation, although it has been argued that this is an unlikely interpretation (*6*). The molecular dynamic studies reported below provide additional evidence that we have correctly assigned four bands to the ester carbonyl group.

Table 2 gives the mean and standard deviation of ester carbonyl integrated absorption intensities for a range of aliphatic esters in three solvents. The standard deviations are quite small, which reflects the uniformity of the absorbances. It is seen that the values for both hexane and acetonitrile are similar, while that for deuterium oxide is significantly lower. We interpret this to mean that the absorbance is more sensitive to hydrogen bonding than to the dielectric constant, since the first two solvents differ significantly in the former category, while deuterium oxide is the only one capable of hydrogen bonding. Hydrogen bonding weakens the dipolar oscillator strength of the carbon−oxygen double bond, upon which the magnitude of the absorbance depends, by drawing electron density toward the hydrogen bond donor. This renders the system more polarizable but less dipolar.

On the assumption that IR absorbance "behaves" in enzyme active sites approximately as it does in homogeneous solutions, we can use the values in Table 2 to estimate how many of the bands seen in Figure 2 represent ester carbonyl vibrations and which may be accordingly assigned to protein perturbation features. We start at the high-frequency side of the spectrum (1746 cm^{-1}) and work down-frequency "filling up" the bands with the absorbance calculated from the model spectra and the protein concentration. These are calculated from the concentration of enzyme, assuming it is all acylated (since there is excess aztreonam present, see the small band at 1762 cm^{-1} in Figure 2) and no deacylation occurs during the experiment. In this process the residual aztreonam band at 1762 cm^{-1} is neglected. We see that the cumulative intensity is 17.7, up to and including the band at 1690 cm^{-1}. The relevant mean intensity of model esters in hexane is 21, and for deuterium oxide it is 14.8. The acyl−enzyme value is thus close to the mean of these values, this being a consequence of the varying dielectric and hydrogen bonding potential as the spectrum is traversed from high to lower frequency. It is perhaps fortunate that the band at 1667 cm^{-1} is large, since there is no surplus absorbance to fill even a portion of this large band after the 1690 cm^{-1} band is filled. This means that we can be confident that the band at 1690 cm^{-1} is the lowest frequency that can be included as an acyl−enzyme carbonyl vibration. Even if one of the bands assigned to acyl−enzyme carbonyl is, in reality, the result of a carboxyl group perturbation (*6*), the 1667 cm^{-1} band could not be included as an acyl−enzyme carbonyl band; its intensity is much too large.

As was the case with the methicillin acyl−enzyme, there are 4 bands in the ester carbonyl region. Several properties of the bands sharply differ from the methicillin spectra, as will be discussed below. Examination of Table 1 reveals that the frequencies of two of the four bands are clearly different between the two difference spectra, while two of the bands are very similar. This leads us to conclude that the method is very sensitive for the detection of conformational distributions and differences between these. Buried carboxyl groups in a hydrophobic environment may be partly protonated, even at neutral pH. Knowles has observed, and decisively assigned by using isotope substitution, a band that arises from protein perturbation at 1748 cm^{-1} in the complex of aldolase with fructose bisphosphate at pD 7.6 (*31*). We have described a similar observation for the acyl−enzymes β-phenylpropionyl− and transcinnamoyl−chymotrypsin, which show perturbation band at 1737 and 1736 cm^{-1}, respectively, albeit at low pH (*4*, *32*). We have previously argued that such an interpretation is unlikely for frequencies below 1735 cm^{-1} and the high-frequency bands (1746 cm^{-1} in the aztreonam spectrum and 1737 cm^{-1} in the methicillin spectrum) that might be susceptible to such interpretation show different frequencies in the two difference spectra. Since quite different

environments for the perturbed carboxyl(s) would need to be invoked in each of the acyl−enzymes, we have reasonable confidence that these bands arise from the ester carbonyl group.

Relative Intensities of the Acyl−Enzyme Carbonyl Bands. In the methicillin spectra the bands were populated, as measured by their intensities, proportionally to the polarity and/or hydrogen bonding of the microenvironment of the carbonyl oxygen. Hydrogen bonding was proposed to stabilize and populate conformers. With aztreonam the conformers are not populated in this way since one with a very nonpolar environment (1746 cm^{-1}) is populated more than 3 times as much as the one seen at 1727 cm^{-1}. The conformer that absorbs at 1690 cm^{-1} has the largest population, and this is presumably the only one that is doubly hydrogen bonded into the oxyanion hole. The interaction is significantly weaker as compared with the methicillin acyl−enzyme (1683 cm^{-1}), and this may represent one reason (apart from a difference in the access of the hydrolytic water molecule) that the deacylation rate is much lower.

Bandwidths of the Acyl−Enzyme Carbonyl Bands. The methicillin acyl−enzyme conformers all have a very similar narrow bandwidth of 10 cm^{-1}; i.e., all conformers are of equivalent well-defined structural/dynamic order. This compares with a width for benzylpenicillin in deuterium oxide of 37 cm^{-1}. With aztreonam, the nonpolar 1746 cm^{-1} conformer has the largest bandwidth, while the others are all similarly narrow and indicate better defined/less mobile conformations, as compared with methicillin. Our studies of model esters revealed that bandwidths are narrowest in hexane and broadest in deuterium oxide; indeed the widths in hexane at high frequency are similar to those of the narrowest acyl−enzyme bands seen at low frequency (1720−1680 cm^{-1}). There is a good linear correlation between the bandwidths and the solvent dielectric constant with correlation coefficient of 0.98 (not shown). This implies that the microenvironment in hexane is isotropic and well defined. As the solvent becomes more polar, and particularly where the possibility of hydrogen bonding is introduced, a variety of rapidly exchanging but discrete dipolar configurations coexist. The structural/dynamic dispersion of the carbonyl group is much higher. Thus, we see that in the enzyme active site this trend is effectively reversed; polarity, which leads to dipolar interaction and hydrogen bonding, reduces the dispersion, as might be expected when the productive configuration is approached. It is important to bear in mind that the reaction channel may be entered from a (presumably even better defined) conformer that is sparsely populated and so invisible in experiments of this type. Such a conformer may represent a near attack complex (*2*). This may be particularly true of kinetically poor complexes such as the aztreonam acyl−enzyme, where the productive conformer is difficult to access owing to steric hindrance of the access of water to the carbonyl. Alternatively reaction may occur slowly from well-populated but poorly aligned complexes.

Role of C3−C4 and N1−C4 Rotations in the Cleaved β-Lactam Ring. The crystal structure of the aztreonem acyl−enzyme showed that the C3−C4 bond of the lactam ring rotates approximately 70° when the ring opens, while the N1−C4 bond rotates approximately 45°; see Scheme 2. This "counterclockwise" rotation leaves the $NHSO_3^-$ moiety in the trajectory for the approach of the incoming hydrolytic water and therefore impairs deacylation. The alternative "clockwise" rotation that would permit facile water approach is prevented by a steric clash between the aztreonam C-4 trans-substituted methyl group and the Tyr-150 and Leu-119 side chains of the protein. Deacylation is very slow, several orders of magnitude slower than for the acyl−enzyme of the aztreonam analogue with the cis-substituted methyl group, which does not clash with the protein during a rotation that clears the incoming path for water; see Scheme 2 (*30*, *33*). The crystal structure of mutant (E166A,Q) class A TEM-1 β-lactamase acylated with benzylpenicillin shows that the anticipated rotation occurs, opening up the approach to the ester bond, although in this case it is not relevant to hydrolysis, since water approaches from the other face (*34*). This rotation would be expected with methicillin to make it a good substrate; however it is a very poor substrate ($k_{deacyl} \approx 0.0001\ s^{-1}$) (*6*). It is possible that unfavorable interactions between the methoxyl substituents of the aromatic acylamino side chain and protein side chains, especially Asn152, a critical element of the catalytic site, might push the acyl moiety into an unfavorable conformation or might cause multiple acyl group conformations that lie off the reaction pathway (*35*).

Scheme 2: Bond Rotations That Occur upon Acylation of *C. freundii* β-Lactamase by Aztreonam[a]

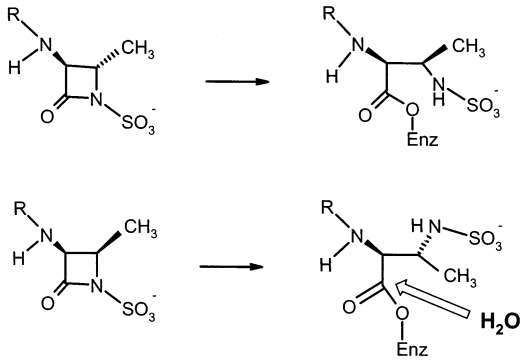

[a] In the acyl−enzyme of the clinically used *trans*-methyl isomer (top) the approach of water is hindered. For the *cis*-methyl isomer deacylation occurs readily as the path for water approach is not hindered.

Changes in the Structure of the Protein on Acylation. The change in the enzyme spectrum upon acylation with aztreonam is quite different from the change seen upon acylation with methicillin, where a change confined to β-sheet was observed (*6*). The spectral features are difficult to assign with certainty, but it is likely that the band at 1667 cm^{-1} represents perturbation of turns, while the predominant band at 1650 cm^{-1} is most likely the consequence of changes in mobile loops (*36*). The small features at 1642 and 1655 cm^{-1} can be assigned to small changes in β-sheet and α-helix, respectively.

Structural Interpretation of the Aztreonam Acyl−Enzyme Conformers. To understand the nature of the four carbonyl entities of the acyl−enzyme species of the *C. freundii* β-lactamase with aztreonam, we resorted to molecular dynamics simulations, starting from the X-ray coordinates of the complex. This complex revealed the carbonyl of the acyl−enzyme species ensconced within the oxyanion hole with two hydrogen bonds to the protein. We have used locally enhanced sampling (LES) to carry out molecular dynamics simulations on this complex. This method, which

is based on a classical version of the time-dependent Hartree approximation (*37*−*41*), has recently been implemented in the AMBER 7 package. The method consists of increasing the computational effort on a region of interest by making multiple copies of the region and in the process increasing statistical sampling, which results in a smoother potential energy surface and more frequent conformational changes (*38*). Recently, Simmerling et al. (*42*, *43*) have applied the method to study systems of biological interest and, in one interesting case (*42*), they were able to find the correct experimental structure of a small RNA tetraloop within a few hundred picoseconds of simulation.

The X-ray structure of the acyl−enzyme intermediate of aztreonam and the class C *C. freundii* β-lactamase shows the ester carbonyl well anchored within the oxyanion hole (*21*). The oxygen of the ester carbonyl is found at 2.8 and 2.7 Å from the main-chain nitrogen atoms of Ser-64 and Ser-318, both within hydrogen-bonding distances. This electrostatic interaction, common to serine proteinases and β-lactamases, is believed to enhance the reactivity of the acyl−enzyme species by both increasing the electrophilicity of the ester carbonyl and stabilizing the tetrahedral species, thus facilitating the deacylation step by an incoming water molecule. The experimental observation of the four species for the ester carbonyl is intriguing. Molecular dynamics represent a powerful tool for the study of the various conformations of the ester carbonyl, since they provide coordinates of atoms and enable one to monitor bond distances, angles, and various other attributes of a system as a function of time.

The distances between the ester carbonyl oxygen and neighboring Ser-64 and Ser-318 backbone nitrogen atoms were monitored over the course of the 1.8 ns simulation. After 60 ps of simulation it was found that aztreonam underwent a conformational change, where the ester carbonyl broke away from the oxyanion hole and pointed toward Tyr-221 (Figure 3 A,B). This configuration of the ester carbonyl remained stable for 150 ps and was followed by the return of the ester carbonyl back to its X-ray crystallographic position. The average distances between carbonyl oxygen and Ser-64 and Ser-318 backbone amide nitrogen atoms were found to be 3.6 and 5.6 Å, respectively, during this sortie from the oxyanion hole. Both these distances are long enough that they preclude the possibility of hydrogen bonding. A similar transition of the ester carbonyl out of the oxyanion hole occurred after 600 ps of simulation. The carbonyl remained out of the oxyanion hole in a similar configuration, for only 50 ps this time, with a subsequent return to the original position in the oxyanion hole. A single structure from the dynamics between 60 and 210 ps of simulation that showed the ester carbonyl out of the oxyanion hole was collected for display in Figure 4 (yellow structure) and was superimposed on the X-ray crystallographic structure (green structure). It is of interest to note that the conformer with the ester carbonyl located out of the oxyanion hole does not form any hydrogen bond interaction with other residues and therefore is clearly in a less polar environment than the carbonyl in the X-ray crystallographic structure. It is likely that the stretching frequency of this conformer corresponds to the signal at 1746 cm^{-1}. Figure 3A,B illustrates the motion of the ester carbonyl in and out of the oxyanion hole during the course of the simulations. Given that carbonyl stretch

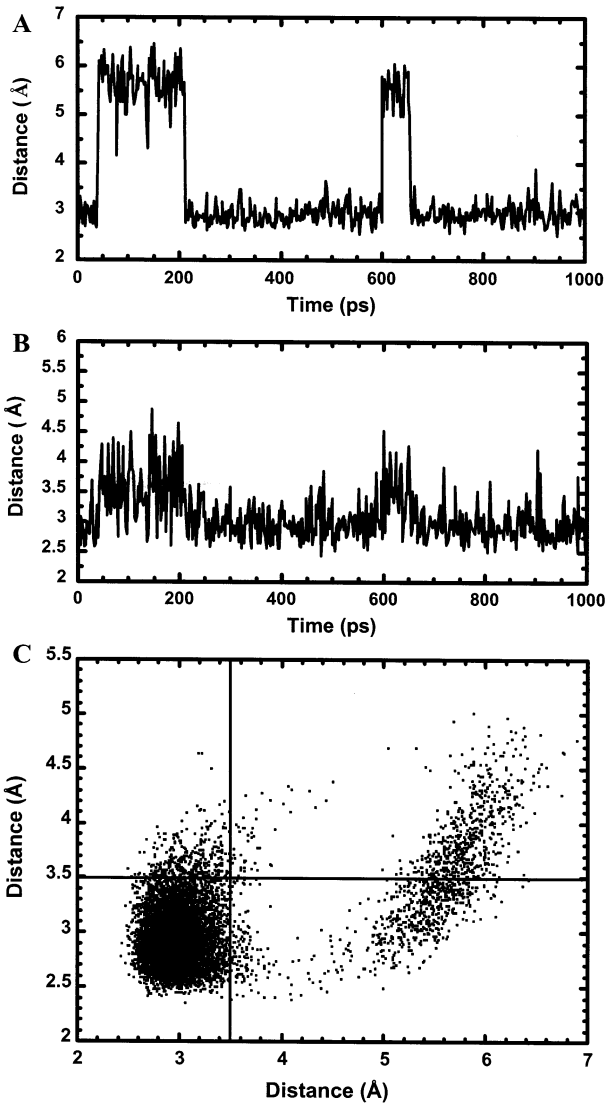

FIGURE 3: (A) Fluctuations in the distance between the ester carbonyl oxygen and the main-chain nitrogen of Ser-318 as a function of time. (B) Fluctuations in the distance between ester carbonyl and the main-chain nitrogen of Ser-64 as a function of time. The data for the trajectory between 1000 and 1800 ps are not shown, as no motion out of the oxyanion hole was detected for that period. (C) Distances between the ester carbonyl oxygen and the main-chain nitrogens of the residue 64 versus those of the residue 318 plotted for the entire 1.8 ns of simulations (a total of 8918 structures).

frequencies were observed between the low-frequency signal (1690 cm^{-1}), attributed to conformers of the ester carbonyl residing in the oxyanion hole, and the high-frequency signal (1746 cm^{-1}), attributed to conformers of the ester carbonyl in a nonpolar environment, it became apparent that conformers with carbonyl in an intermediate environment are likely to be responsible for the IR signals between the highest and lowest carbonyl stretch frequencies.

The distances between the ester carbonyl oxygen and the backbone amide nitrogen of Ser-64 are plotted against the distances between the ester carbonyl and the backbone amide nitrogen of Ser-318, as shown in Figure 3C for structures collected over the course of the trajectory. Vertical and horizontal lines are drawn at 3.5 Å to represent the distance at which hydrogen-bonding interaction does not exist. The bottom left quadrant corresponds to conformers with the ester

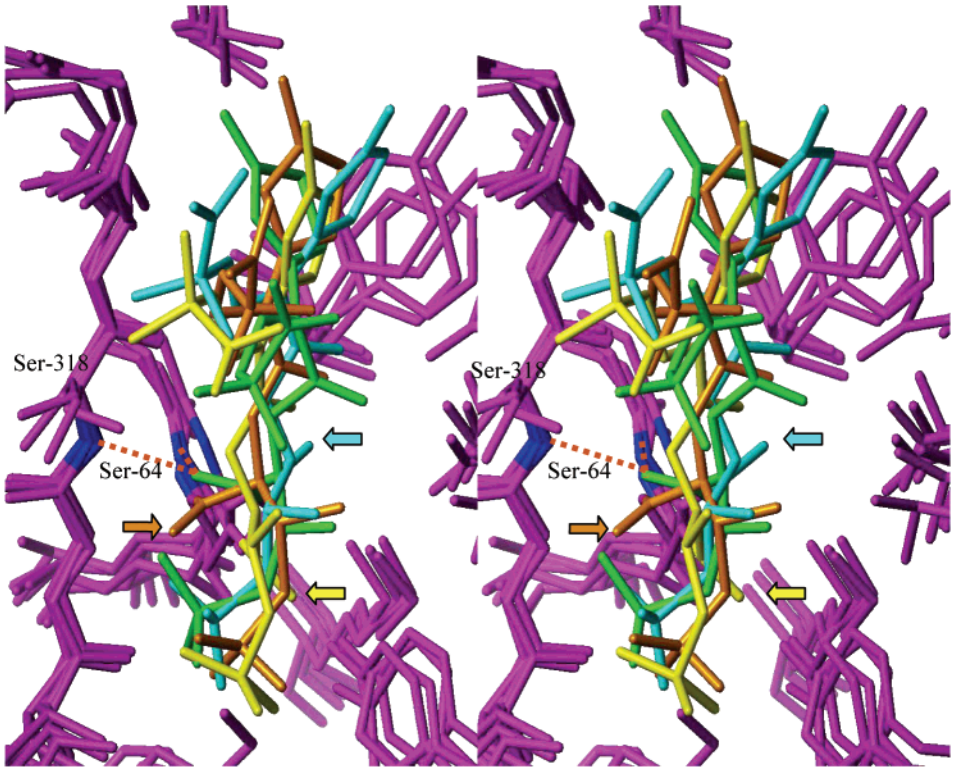

FIGURE 4: Stereoimages of the superimposition of the X-ray structure for the acyl−enzyme species (in green) and three structures from the course of the simulation. A structure with both hydrogen bonds broken is in yellow, one structure with a hydrogen bond to Ser-64 is depicted in cyan, and one structure with a hydrogen bond to Ser 318 is shown in orange. The color-coded arrows point to the ester carbonyl oxygen in each case.

carbonyl residing in the oxyanion hole, which is most populated. The upper right quadrant contains conformers with both hydrogen bonds (to Ser-64 and to Ser-318) broken. As stated earlier, these conformers correspond to the ester carbonyl residing out of the oxyanion hole in a nonpolar microenvironment. The lower right and upper left quadrants correspond to species where the ester carbonyl retains one hydrogen bond with either Ser-64 or Ser-318. We propose that these species are likely responsible for the IR signals measured at 1708 and 1727 cm^{-1}. The lower frequency signal at 1708 cm^{-1} signifies that the carbonyl corresponding to this conformer resides in a more polar environment as compared with the species represented by the signal at 1727 cm^{-1}. As a result, the lower frequency signal is likely to correspond to conformers hydrogen bonded to Ser-318, given that this interaction is stronger. Whereas the methodology applied to dynamic simulations is state of the art, the distributions of these conformers do not correspond to the integration of the signals for the IR experiment, since the duration of the simulation does not approach that for the data collection by IR. Nonetheless, the simulations provide critical insights into the likely events that take the carbonyl of the acyl−enzyme species from one extreme (ensconced in the oxyanion hole) to another (entirely out of the oxyanion hole) via intermediary structures.

SUMMARY

It is now clear that X-ray crystallographic structures may present an incomplete picture of the conformational distribution of bound ligands in the solution phase, particularly perhaps where the complex is geometrically suboptimal. We have previously shown that the natural product antibiotic benzylpenicillin occupies a single well-defined conformation when interacting in acyl−enzyme form with a susceptible (*S. pneumoniae*, PBP2x) transpeptidase target (*44*). This interaction has been optimized over the course of evolution. However, we have also shown that the aztreonam acyl−enzyme formed with PBP2x has a single conformation (C.W.W., unpublished observation). It thus appears that transpeptidases and β-lactamases handle β-lactams differently. For effective inhibitors of transpeptidases, such as aztreonam, the acyl−enzyme formed is a stable well-defined singular complex. For poor substrates of β-lactamases, such as aztreonam and methicillin, a less well ordered complex with multiple conformers is favored, in which the approach of water is also restricted. The test of this hypothesis, not yet experimentally viable, will be the measurement of the IR spectra of the highly specific (and very transient) acyl−enzymes formed by the interaction of e.g. cephalosporin c with the *C. freundii* enzyme or benzylpenicillin with the *E. coli* TEM-1 enzyme. We would expect a single well-defined conformer to be observed.

The implications of the existence of conformational multiplicity for future drug design may be significant; it is possible that, in addition to impeding water access, compounds can be designed to make use of unfavorable interactions with the protein that result in inactive conformers at the acyl−enzyme stage (*18*).

The powerful combination of computer simulation with IR spectroscopy and X-ray crystallography now provides a structural dimension to the interpretation of IR spectra. This adds significantly to the value of the IR method, which will be further strengthened when quantum mechanical calculations of the IR frequencies are completed. When this is

achieved, we expect that it will be possible to invert the procedure and deduce structures directly from IR spectra, provided a crystal or NMR structure is available for the parent (unliganded) protein.

ACKNOWLEDGMENT

We thank Simon Ward for expert technical assistance with IR spectroscopy.

REFERENCES

1. Bode, W., and Huber, R. (1992) *Eur. J. Biochem. 204*, 433−451.
2. Bruice, T. C., and Benkovic, S. J. (2000) *Biochemistry 39*, 6267−6275.
3. Eads, J., Sacchettini, J. C., Kromminga, A., and Gordon, J. I. (1993) *J. Biol. Chem. 268*, 26375−26385.
4. White, A. J., Drabble, K., and Wharton, C. W. (1992) *Biochem. J. 287*, 317−323.
5. White, A. J., and Wharton, C. W. (1990) *Biochem. J. 270*, 627−637.
6. Wilkinson, A.-S., Ward, S., Kania, M., Page, M. G. P., and Wharton, C. W. (1999) *Biochemistry 38*, 3851−3856.
7. Polshakov, V. I., Birdsall, B., and Feeney, J. (1999) *Biochemistry 38*, 15962−15969.
8. Falzone, C. J., Wright, P. E., and Benkovic, S. J. (1991) *Biochemistry 30*, 2184−2191.
9. Citri, N., and Zyk, N. (1982) *Biochem. J. 201*, 425−427.
10. Citri, N., Kalkstein, A., Samuni, A., and Zyk, N. (1984) *Eur. J. Biochem. 144*, 333−338.
11. Taibi, P., and Mobashery, S. (1995) *J. Am. Chem. Soc. 117*, 7600−760.
12. Taibi-Tronche, P., Massova, I., Valulenko, S. B., Lerner, S. A., and Mobashery, S. (1996) *J. Am. Chem. Soc. 118*, 7441−7448.
13. Maveyraud, L., Massova, I., Birck, C., Miyashita, K., Samama, J.-P., and Mobashery, S. (1996) *J. Am. Chem. Soc. 118*, 7435−7452.
14. Maveyraud, L., Mourey, L., Kotra, L. P., Pedelacq, J.-D., Guillet, V., Mobashery, S., and Samama, J.-P. (1998) *J. Am. Chem. Soc. 120*, 9748−9752.
15. Wharton, C. W. (2000) *Nat. Prod. Rep. 17*, 447−454.
16. Vakulenko, S. B., Taibi-Tronche, P., Tóth, M.; Massova, I., Lerner, S. A., and Mobashery, S. (1999) *J. Biol. Chem. 274*, 23052−23060.
17. Meroueh, S. O., Roblin, P., Golemi, D., Maveryraud, L., Vakulenko, S. B., Zhang, Y., Samama, J. P., and Mobashery, S. (2002) *J. Am. Chem. Soc. 124*, 9422−9430.
18. Swarén, P., Massova, I., Bellettini, J., Bulychev, A., Maveyraud, L., Kotra, L. P., Miller, M. J.; Mobashery, S., and Samama, J. P. (1999) *J. Am. Chem. Soc. 121*, 5353−5359.
19. Fink, A. L., Ellerby, L. M., and Bassett, P. M. (1989) *J. Am. Chem. Soc. 111*, 6871−6873.
20. Kotra, L. P., Samama, J. P., and Mobashery, S. (2002) Structural Aspects of β-Lactamase Evolution, in *Bacterial Resistance to Antimicrobials, Mechanisms, Genetics, Medical Practice and Public Health* (Lewis, A., Salyers, Haber, H., and Wax, R. G., Eds.) pp 123−159, Marcel Dekker, New York.
21. Oefner, C., Darcy, A., Daly, J. J., Gubernator, K., Charnas, R. L., Hubschwerlen, C., and Winkler, F. K. (1990) *Nature 343*, 284−288.
22. Case, D. A., Pearlman, D. A., Caldwell, J. W., Cheatham, T. E., III, Wang, J., Ross, W. S., Simmerling, C. L., Darden, T. A., Merz, K. M., Stanton, R. V., Cheng, J. J., Vincent, A. L., Crowley, M., Tsui, V., Gohlke, H., Radmer, R. J., Duan, Y., Pitera, J., Massova, I., Seibel, G. L., Singh, U. C., Weiner, P. K., and Kollman, P. A. (2002). *AMBER 7*, University of California, San Francisco, CA.
23. Bayly, C. I., Cieplak, P., Cornell, W. D., and P. A. Kollman (1993) *J. Chem. Phys. 97*, 10269.
24. Frisch, M. J., Trucks, G. W., Schlegel, H. B., Scuseria, G. E., Robb, M. A., Cheeseman, J. R., Zakrzewski, V. G., Montgomery, J. A., Jr., Stratmann, R. E., Burant, J. C., Dapprich, S., Millam, J. M., Daniels, A. D., Kudin, K. N., Strain, M. C., Farkas, O., Tomasi, J., Barone, V., Cossi, M., Cammi, R., Mennucci, B., Pomelli, C., Adamo, C., Clifford, S., Ochterski, J., Petersson, G. A., Ayala, P. Y., Cui, Q., Morokuma, K., Malick, D. K., Rabuck, A. D., Raghavachari, K., Foresman, J. B., Cioslowski, J., Ortiz, J. V., Stefanov, B. B., Liu, G., Liashenko, A., Piskorz, P., Komaromi, I., Gomperts, R., Martin, R. L., Fox, D. J., Keith, T., Al-Laham, M. A., Peng, C. Y., Nanayakkara, A., Gonzalez, C., Challacombe, M., Gill, P. M. W., Johnson, B. G., Chen, W., Wong, M. W., Andres, J. L., Head-Gordon, M., Replogle, E. S., and Pople, J. A. (1998) *Gaussian 98*, revision A.6, Gaussian, Inc., Pittsburgh, PA.
25. Maveyraud, L., Golemi, D., Ishiwata, A., Meroueh, O., Mobashery, S., and Samama, J.-P. (2002) *J. Am. Chem. Soc. 124*, 2461−2465.
26. Darden, T. A., York, D. M., and Pedersen, L. G. (1993) *J. Chem. Phys. 98*, 10089−10092.
27. Ryckaert, J. P., Ciccotti, G., and Berendsen, J. H. C. (1977) *J. Comput. Chem. 23*, 327−331.
28. Simmerling, C. L., Miller, J. L., and Kollman, P. A. (1998) *J. Am. Chem. Soc. 120*, 7149−7155.
29. Galleni, M., and Frere, J.-M. (1988) *Biochem. J. 255*, 123−129.
30. Heinze-Krauss, I., Anghern, P., Charnas, R. L., Gubernator, K., Gutnecht, E.-M., Hubscwerlen, C. M., Kania, M., Oefner, C., Page, M. G. P., Sogabe, S., Specklin, J.-L., and Winkler, F. (1998) *J. Med. Chem. 41*, 3961−3971.
31. Fisher, J., Belasco, J. G., and Knowles, J. R. (1980) *Biochemistry 19*, 2895−2993.
32. Johal, S. S., White, A. J., and Wharton, C. W. (1994) *Biochem. J. 297*, 281−287.
33. Matsuda, K., Sanada, M., Inoue, M., and Mitashashi, S. (1991) *Antimicrob. Agents Chemother. 35*, 458−461.
34. Strynadka, N. C. J., Adachi, H., Jensen, S. E., Johns, K., Sielecki, A., Betzel, C., Sutoh, K., and James, M. N. G. (1990) *Nature 359*, 700−705.
35. Dubus, A., Normark, S., Kania, M., and Page, M. G. P. (1995) *Biochemistry 34*, 7757−7764.
36. Arrondo, J.-L. R., and Goni, F. M. (1999) *Prog. Biophys. Mol. Biol. 72*, 367−405.
37. Elber, R., and Karplus, M. (1990) *J. Am. Chem. Soc. 112*, 9161−9175.
38. Roitberg, A., and Elber, R. (1991) *J. Chem. Phys. 95*, 9277−9287.
39. Straub, J. E., and Karplus, M. (1991) *J. Chem. Phys. 94*, 6737−6739.
40. Ulitsky, A., and Elber, R. (1993) *J. Chem. Phys. 98*, 3380−3388.
41. Zheng, Q., Rosenfeld, D. J., and J. Kyle (1993) *J. Chem. Phys. 99*, 8892−8896.
42. Simmerling, C. L., Miller, J. L., and Kollman, P. A. (1998) *J. Am. Chem. Soc. 120*, 7149−7155.
43. Simmerling, C. L., Lee, M. R., Ortiz, A. R., Kolinski, A., Skolnick, J., and Kollman, P. A. (2000) *J. Am. Chem. Soc. 122*, 8392−8402.
44. Chittock, R. S., Ward, S., Wilkinson, A.-S., Caspers, P., Mensch, B., Page, M. G. P., and Wharton, C. W. (1999) *Biochem. J. 338*, 153−159.

BI0266941